Photochemical & Photobiological Sciences

RSC Publishing

PAPER

Synthesis and photopolymerization kinetics of benzophenone sesamol one-component photoinitiator

Cite this: *Photochem. Photobiol. Sci.*, 2013, **12**, 323

Jinliang Yang,[a] Suqing Shi,[b] Fei Xu[a] and Jun Nie*[a]

Received 2nd July 2012,
Accepted 19th September 2012

DOI: 10.1039/c2pp25241d

www.rsc.org/pps

A benzodioxole derivative, 4-(2-(benzodioxol-5-yloxy)ethoxy)benzophenone (BPC2BDO), based on 4-hydroxybenzophenone and sesamol was synthesized, and used as a one-component Type II photoinitiator. The structure of BPC2BDO was characterized by elementary analysis, APCI-MS, ^{1}H NMR, and ^{13}C NMR. The rate of decomposition (R_d) of BPC2BDO in acetonitrile was studied by UV-Vis spectroscopy and found that R_d was proportional to light intensity. Real-time near-IR was used to study the kinetics of photopolymerization of the photoinitiator. As the benzophenone (BP) moiety and hydrogen donor were introduced into one molecule in BPC2BDO, radicals could be generated through intra-molecular reaction due to the close vicinity of the hydrogen donor and BP, which might be faster than inter-molecular reaction. The results also showed that the rate of polymerization of acrylates was significantly higher than that of methacrylates at the same polymerization conditions; the functionality of acrylates, concentration of BPC2BDO, and light intensity affected the polymerization rate and the final conversion.

1 Introduction

Photopolymerization has drawn extensive attention in the last few decades because of its greater advantages including high efficiency, low energy consumption, and environmental issues.[1] It is an effective industrial process which is widely used in various applications such as inks, adhesives, coating, optical waveguides, and microelectronics.[1–5] The majority of efforts have been dedicated to photo-initiated free radical systems because the widely used monomers and the photoinitiators having sensitivity in both UV and visible range.[6,7]

A Type II photoinitiator system is one in which initiating free radicals are formed by a bimolecular process consisting of a triplet excited state of an aromatic carbonyl compound and a hydrogen donor compound as a co-initiator. Benzophenone (BP) and its derivatives,[8] thioxanthones,[9] benzil,[10] quinones,[10] and organic dyes[11] are typical examples of Type II photoinitiators. Based on their hydrogen-donating capability, alcohols, amines, ethers, and thiols are used as co-initiators.

Benzophenone is one of the most widely used photoinitiators due to its good surface curing, oxygen inhibition effect, and solubility properties, together with the high quantum efficiency of the hydrogen abstraction particularly with amines.[12,13] In the BP photopolymerization process, the photopolymerization of acrylates or methacrylates are usually initiated by the radicals produced from the hydrogen donor.[14,15] The ketyl radicals are usually not effective in initiating free-radical polymerization due to the steric hindrance and the delocalization of unpaired electrons.[16] However, using small molecular weight tertiary amines as co-initiators in formulations is not only prone to lead to yellowing,[17] but they are also toxic and mutagenic.[18] Although greater molecular weight amines[19,20] or polymerizable amines[21,22] are synthesized to further enhance the biocompatibility of the co-initiator, seeking a more biocompatible co-initiator is still a great challenge.

Benzodioxole derivatives, natural components from dietary plants such as peppers, sesame seeds and carrots,[23–25] found in a wide variety of human food, essential oils and flavors, could be used as hydrogen donors instead of amine for bimolecular photoinitiating systems. The benzodioxole derivatives possess antioxidant, antibacterial, antifungal, and other biological activities.[24–27] In particular, the very low mammalian toxicity is of great interest.[28] A typical example includes a natural component, 1,3-benzodioxole, which replaced conventional hazardous amine co-initiators for dental applications.[29,30]

In our previous study[31] we found that the introduction of the electron-donating substituents in the 5-position of 1,3-benzodioxole contributed to an increase in the reactivity of the BP/benzodioxole-based system, however electron-withdrawing substituents in the same position caused the opposite effect.

[a]*State Key Laboratory of Chemical Resource Engineering, Beijing University of Chemical Technology, Beijing 100029, P.R. China. E-mail: niejun@mail.buct.edu.cn; Fax: (+86) 10-6442-1310; Tel: (+86) 10-6442-1310*

[b]*Key Laboratory of Synthetic and Natural Functional Molecule Chemistry of Ministry of Education and College of Chemistry and Materials Science, Northwest University, Xi'an 710069, P.R. China. E-mail: shisq@nwu.edu.cn; Fax: (+86) 29-8830-3845; Tel: (+86) 29-8830-3845*

As a part of our continuing interest in the design and development of photoinitiating systems, and the expansion of their use in photopolymerization, we report herein the use of 4-(2-(benzodioxol-5-yloxy)ethoxy)benzophenone (BPC2BDO) as a one-component Type II photoinitiator.

2 Experimental

2.1 Materials

Benzophenone (BP) and 4-hydroxybenzophenone (HBP) were obtained from Runtec Co. (Jintan, Jiangsu, China). Sesamol was purchased from Wuhan Yuancheng Technology Development Co. Ltd. (Wuhan, Hubei, China). The monomers were all obtained from Sartomer Company (Warrington, PA, USA). Dichloromethane and acetonitrile were dried and purified according to common laboratory methods.[32] All other reagents were of analytical grade and used as received without further purification. Chemical structures of the monomers are shown in Scheme 1.

2.2 Synthesis

The synthesis route of BPC2BDO is outlined in Scheme 2.

2.2.1 Synthesis of 5-(2-chloroethoxy)benzodioxole (BDOCl). A mixture of sesamol (13.81 g, 0.1 mol), sodium hydroxide (8.00 g, 0.2 mol) and water (75 mL) were stirred together for 1 h in a three-necked flask equipped with stirrer, thermometer, and dropping funnel. Tetrabutyl ammonium bromide (3.20 g, 14.6 mmol) dissolved in 75 mL of 1,2-dichloroethane was added dropwise over 30 min. The mixture was refluxed for 24 h. After the reaction mixture was cooled to room temperature, the upper aqueous layer was removed. The organic layer was dried overnight by anhydrous sodium sulfate and evaporated under reduced pressure to afford a brown solid. The crude product was purified by column chromatography with dichloromethane as eluent to obtain a white solid. Yield: 16.60 g (83%).

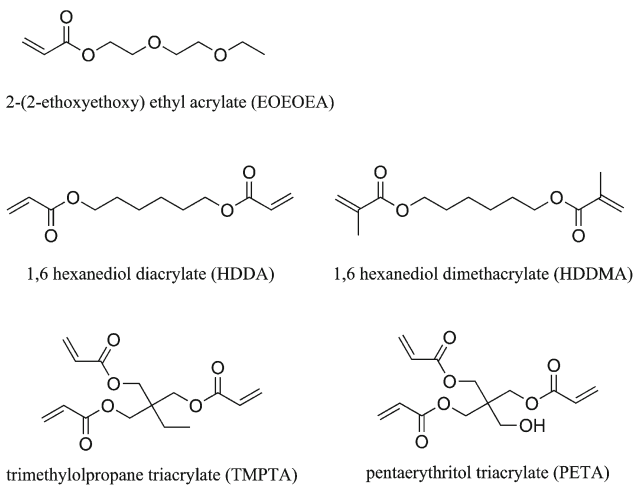

Scheme 1 Chemical structures of monomers.

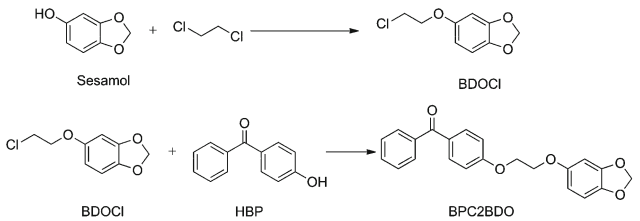

Scheme 2 The synthesis route of BPC2BDO.

^{1}H NMR (400 MHz, $CDCl_3$) δ (ppm): 6.69–6.72 (1H, Ar*H*), 6.51–6.53 (1H, Ar*H*), 6.33–6.36 (1H, Ar*H*), 5.92 (2H, –O–C*H*$_2$–O–), 4.14–4.17 (2H, –O–C*H*$_2$–), 3.76–3.79 (2H, –C*H*$_2$–Cl).

^{13}C NMR (400 MHz, $CDCl_3$) δ (ppm): 153.63, 148.35, 142.25, 107.98, 106.22, 101.26, 98.60, 69.18, 41.91.

2.2.2 Synthesis of (BPC2BDO). Anhydrous potassium carbonate (4.10 g, 30 mmol) was added to the solution of 4-hydroxybenzophenone (1.98 g, 10 mmol) in 60 mL of acetonitrile at room temperature under a nitrogen atmosphere. The mixture was stirred vigorously for 2 h. 2.00 g (10 mmol) of BDOCl dissolved in 10 mL of acetonitrile was added dropwise, then the mixture was allowed to reflux for 24 h. After the reaction mixture was cooled to room temperature, the precipitate was filtered off and washed 3 times with 10 mL acetonitrile. The organic layers were combined and the solvent was removed under vacuum to afford a brown solid. The crude product was further purified by column chromatography with dichloromethane as eluent to afford BPC2BDO as a white solid. Yield: 1.38 g (38%).

Anal. calcd for $C_{18}H_{22}O_5$: C, 72.92; H, 5.01%. Found: C, 72.86; H, 5.02%.

Q-Tof-MS (*m*/*z*): calcd for $C_{18}H_{22}O_5$, 362.1154. Found: 363.1230 $[M + H]^+$.

^{1}H NMR (400 MHz, $CDCl_3$) δ (ppm): 7.83–7.85 (2H, Ar*H*–CO–), 7.75–7.77 (2H, –CO–Ar*H*–O–), 7.55–7.59 (1H, Ar*H*–CO–), 7.46–7.50 (2H, Ar*H*–CO–), 7.00–7.02 (2H, –CO–Ar*H*–O–), 6.71–6.73 (1H, Ar*H*), 6.55–6.56 (1H, Ar*H*), 6.37–6.40 (1H, Ar*H*), 5.93(2H, –O–C*H*$_2$–O–), 4.36–4.38 (2H, –O–C*H*$_2$–CH$_2$–O–), 4.29–4.30 (2H, –O–CH$_2$–C*H*$_2$–O–).

^{13}C NMR (400 MHz, $CDCl_3$) δ (ppm): 195.54, 162.25, 153.99, 148.34, 142.12, 138.23, 132.56, 131.94, 130.54, 129.75, 128.21, 114.19, 107.96, 106.01, 101.24, 98.48, 67.41, 66.74.

2.3 Instrumentation

The compositions of C, H were determined with Vario EL cube (Elementar Analysensysteme, Germany), equipped with Mettler-Toledo XP6 (Mettler-Toledo GmbH, Germany) in CHNS operation mode.

The ACPI-MS experiments were carried out by using a Xevo G2 Q-Tof mass spectrometer (Waters, MA, USA) equipped with an atmospheric pressure chemical ionization interface. The instrument was calibrated with leucine enkephalin in the mass range of 50–1200 amu.

The ^{1}H and ^{13}C NMR spectra were carried out on a 400 MHz NMR instrument (Bruker Corporation, Germany) at 298 K with $CDCl_3$ as solvent and TMS as internal standard.

The UV-Vis absorption spectra were recorded on a Hitachi U-3010 UV-Vis spectrophotometer (Hitachi High-Technologies Corporation, Tokyo, Japan) at room temperature using acetonitrile as solvent.

The ESR spectra were run on a Jeol JES-FA200 X-band ESR spectrometer(JEOL Ltd., Tokyo, Japan) in acetonitrile at 298 K.

2.4 Photoreduction

Photoreduction of BPC2BDO was studied by using UV absorption spectroscopy. BPC2BDO was dissolved in acetonitrile and the solution was deoxygenated by bubbling nitrogen into the solution for 30 min. The relative rate of photoreduction was determined by measuring the decrease in the peak absorbance of BPC2BDO at 286 nm with irradiation time. The rate of decomposition (R_d) of BPC2BDO photoinitiator (PI) was calculated according to the following equation:

$$R_d = -d[PI]/dt = -([BPC2BDO]/Ab_0) \times (d(Ab)/dt) \quad (1)$$

where Ab_0 and Ab are the absorbance of BPC2BDO at 286 nm before and after exposure to UV light.

2.5 ESR spin-trapping experiments

ESR spin-trapping experiment was carried out using a Jeol JES-FA200 X-band spectrometer at 100 kHz magnetic field modulation. The radicals were generated under the polychromatic light exposure of an Hg–Xe lamp (Hamamatsu L8252, 150 W). The acetonitrile solutions with BPC2BDO were added to Quartz cylindrical ESR tubes and were deoxygenated with argon for 15 min before measurements. The radicals generated in by the photoinitiator were trapped by phenyl-*N*-*tert*-butylnitrone (PBN).

2.6 Photopolymerization kinetics

The mixtures of monomer and one-component photoinitiator were injected into a mold made from glass slides and spacers with 15 ± 1 mm diameter and 2 ± 0.1 mm thickness, irradiated by a UV spot light source (EFOS Lite, 100 W miniature arc lamp with 320–500 nm filter and 5 mm crystal optical fiber, Canada) at room temperature. The light intensity was determined by a UV-light Radiometer (Beijing Normal University, China).

The kinetics of photopolymerization was studied by the real-time near-IR (RT-NIR) spectrometer. The spectrometer (Nicolet 5700) equipped with a MCT/A KBr detector-beam splitter combination was used to monitor the photopolymerization kinetics. The spectrometer was operated in the absorbance mode, and the polymerization kinetics was determined by the RT-NIR spectrometer working in the rapid mode with an average 4 scans s^{-1} collection rate (4 cm^{-1}) and calculated by the decrease of the area of (meth)acrylate double bond absorption peak around 6162 cm^{-1}.[33] The double-bond conversions (DC), directly related to the decrease in NIR absorbance, was calculated from eqn (2):

$$DC\% = \left[1 - \frac{(A_{6162})_t}{(A_{6162})_0}\right] \times 100\% \quad (2)$$

where $(A_{6162})_0$ and $(A_{6162})_t$ are the areas of the NIR absorption peak at 6162 cm^{-1} of the sample before and after photopolymerization at time t, respectively. Correspondingly, the actual polymerization rate (R_p) was obtained from eqn (3):

$$R_p(s^{-1}) = \frac{d(DC_t)}{dt} \Big/ (A_{6162})_0 \quad (3)$$

where DC_t is the double-bond conversions of polymerization at time t.

3 Results and discussion

3.1 UV spectroscopy

UV absorption spectrum of BPC2BDO in acetonitrile was measured while the equimolar BP was considered as reference. The maximum absorption (λ_{max}) and the molar extinction coefficient at λ_{max} (ε_{max}) are summarized in Table 1.

Fig. 1 shows the UV absorption spectra of BPC2BDO and BP. For BP, the absorptions in the region of 250 nm and 338 nm were attributed to its π–π* transition and n–π* transition, respectively. Although the n–π* transition at 338 nm was the symmetry forbidden transition, the (n, π*) excited states were known to be more reactive than (π, π*) excited states towards hydrogen abstraction. Compared with BP, the absorption maximum of BPC2BDO was found at 286 nm, which exhibited a significant red-shift of the π–π* type (36 nm) because of the hetero-linker.[13] Therefore, the n–π* transition was overlaid by the shoulder of the more intense π–π* transition at higher concentrations.

Table 1 UV absorption data of photoinitiators (PI) in acetonitrile

PI	λ_{max} (nm)	ε_{max} (L mol^{-1} cm^{-1})
BP	250	17 750
	338	126
BDOCBP	286	20 898
	338	350

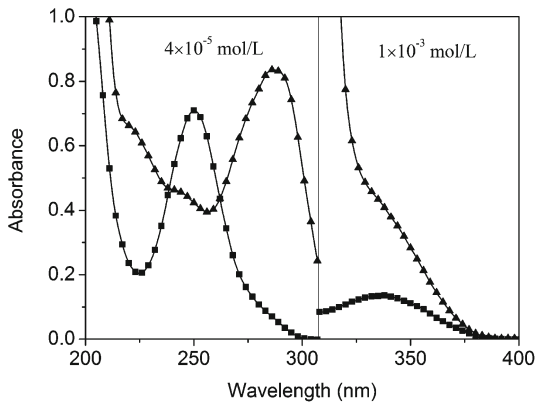

Fig. 1 UV absorption spectra of BPC2BDO (▲) and BP (■) in acetonitrile solution (4.0×10^{-5} and 1.0×10^{-3} mol L^{-1}).

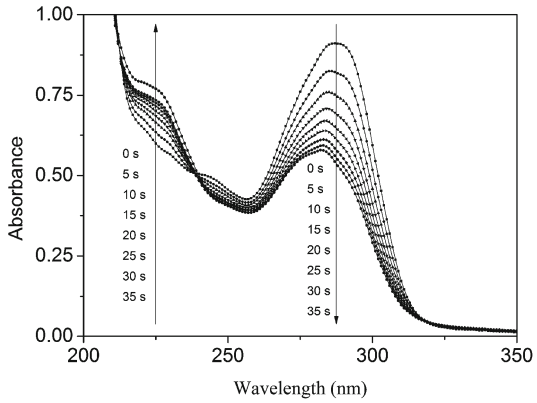

Fig. 2 Typical UV spectra change of BPC2BDO in acetonitrile by UV irradiation under nitrogen ([BPC2BDO] = 4.3 × 10^{-5} mol L^{-1}, I = 25 mW cm^{-2}).

3.2 Photoreduction

Photoreduction studies were conducted from 0 to 35 s at intervals of 5 s with constant UV light intensity 25 mW cm^{-2}. During the UV light irradiation of BPC2BDO in acetonitrile, the absorption of BPC2BDO at 286 nm decreased as shown in Fig. 2. At the end of the irradiation, the absorbance at 286 nm was reduced from 0.91 to 0.55.

The rate of the initiator decomposition (R_d) could be expressed as follows:[2]

$$R_d = \Phi I_a = \Phi I_0(1 - e^{-\varepsilon c l}) \quad (4)$$

where: I_0 is intensity of incident light, Φ is quantum yield for production of radicals, ε is molar absorptivity of initiator at the wavelength employed, c is initiator concentration, l is path length, and I_a is absorbed intensity.

Assuming the validity of the Beer–Lambert law, eqn (4) could be expressed as follows:

$$\ln(e^{2.303A_0} - 1) - \ln(e^{2.303A_t} - 1) = 2.303\Phi I_0 \varepsilon t \quad (5)$$

where A_0 and A_t are the heights of the absorption of BPC2BDO at 286 nm before and after irradiation at time t, respectively.

The decrease in the maximum absorbance of BPC2BDO at 286 nm in the presence of different light intensities is presented in Fig. 3a. It can be seen that $\ln(e^{2.303A_t} - 1)$ fitted a straight line *versus* the irradiation time at different light intensities (Fig. 3b); the correlation coefficients inferred that the relationship of $\ln(e^{2.303A_t} - 1)$ and the irradiation time at different light intensities matched eqn (5) well.

Theoretically, R_d of the photoinitiator is linearly related to light intensity (seen in eqn (4)). In Fig. 3c, it could be observed that the R_d of BPC2BDO had good linear relationship with light intensity (r^2 = 0.99) when the light intensity was relatively lower. However, when the solution of BPC2BDO was irradiated with higher light intensity (*i.e.* 25 mW cm^{-2}), the obtained R_d value was relatively lower than that of theoretical one. It indicated that, at lower light intensity, the intramolecular hydrogen abstraction was predominant. When the solution of one-component Type-II photoinitiator BPC2BDO was exposed

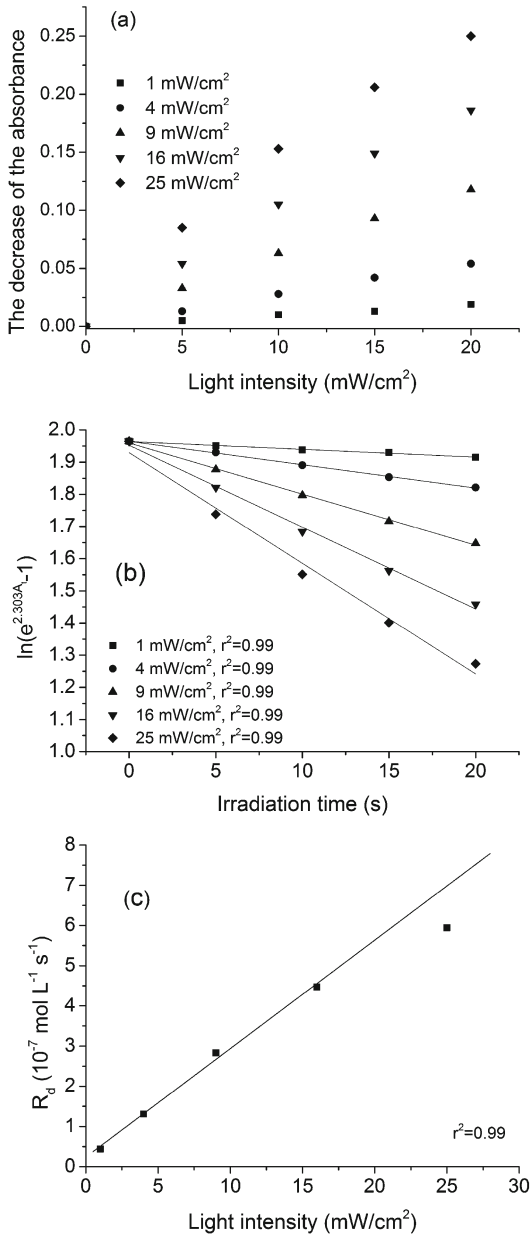

Fig. 3 Photoreduction characteristics of BPC2BDO at 286 nm. (a) The decrease of the absorbance *vs.* irradiation time; (b) $\ln(e^{2.303A_t} - 1)$ *vs.* irradiation time; (c) R_d *vs.* light intensity ([BPC2BDO] = 4.3 × 10^{-5} mol L^{-1}).

to irradiation with higher light intensity, the more excited BPC2BDO resulted in the occurrence of the intramolecular and intermolecular hydrogen abstraction at the same time, which might cause the deviation from the linear relationship.

3.3 ESR experiments

ESR spin trapping (ESR-ST) experiments were performed to characterize the radicals generated in the photoinitiator systems using PBN as spin trap.[34–36] An example ESR spectrum for BPC2BDO is given in Fig. 4. The hyperfine splitting constants (HFS) for both the nitrogen (a_N) and the hydrogen (a_H) of the spin adducts are gathered in Table 2.

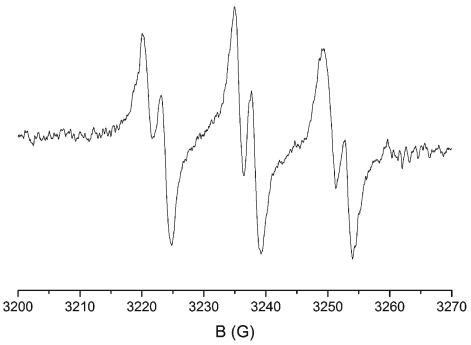

Fig. 4 ESR spectrum of the radical generated in BPC2BDO and trapped by PBN.

Table 2 HFS Values of the radicals observed in the ESR-ST experiments

Photoinitiating system	a_N (G)	a_H (G)
BP/EDAB	15.08	2.34
BP/BDO	14.99	2.60
BPC2BDO	14.95	3.01

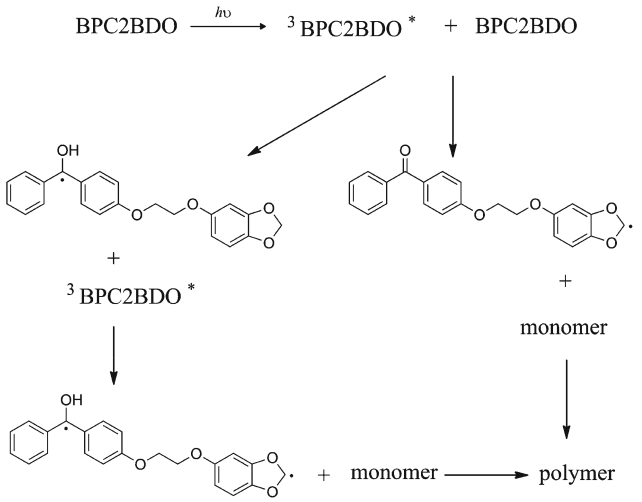

Scheme 3 Proposed mechanism of the radical formation with BPC2BDO.

On the basis of the these experiments, the photochemical mechanism of the radical formation in BPC2BDO is illustrated in Scheme 3. It appears that the BPC2BDO-derived methine radical could be generated from the interaction between the triplet BPC2BDO and the cyclic acetal group of BPC2BDO, which means that BPC2BDO could be used as a one-component Type II photoinitiator. The generation of radicals through a direct hydrogen abstraction between BPC2BDO and the monomer (as in BP alone) can contribute to some extent.

3.4 The comparison of BPC2BDO and BP/BDO as photoinitiator

Plots of double bond conversions *vs.* irradiation time for the polymerization of HDDA induced by BPC2BDO and BP/BDO are shown in Fig. 5a. Because they had the same molar concentration of the BP moiety, the final conversion of BPC2BDO was almost the same as that of BP/BDO but the polymerization rate was slightly higher than that of BP/BDO (Fig. 5b). As the BP moiety and BDO were introduced in one molecule in BPC2BDO, the radicals could be generated through intra-molecular reaction due to the close vicinity of the hydrogen donor and BP, which might be faster than inter-molecular reaction.[12] Moreover, the introduction of the electron-donating substituents in the 5-position of 1,3-benzodioxole could also increase the reactivity of BP/benzodioxole-based system.[31] These results indicated that BPC2BDO was a more effective photoinitiator than BP/BDO.

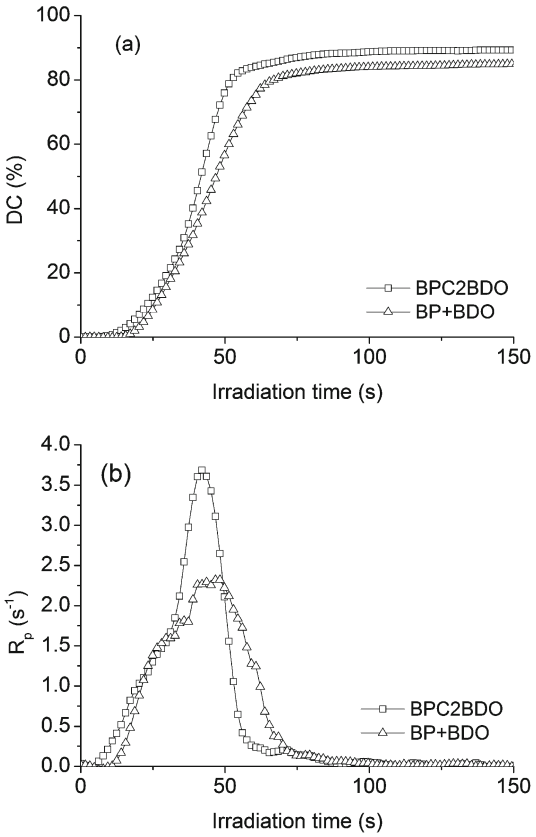

Fig. 5 Double bond conversions (a) and R_p (b) *vs.* irradiation time for the polymerization of HDDA induced by BPC2BDO and BP/BDO (I_0 = 30 mW cm^{-2}, [BPC2BDO] = [BP] = [BDO] = 2.76 × 10^{-5} mol g^{-1}).

3.5 The influencing factors on photopolymerization

HDDA was chosen as the monomer for further studies of the one-component photoinitiator because it has moderate viscosity and reactivity.

Plots of DC *versus* irradiation time for HDDA with different BPC2BDO concentrations in the initiating system are shown in Fig. 6a. The polymerization rate and final conversion increased with increase of BPC2BDO concentration. Because higher BPC2BDO concentration could produce more free radicals during irradiation, it caused the higher rate of polymerization. On the other hand, this might be due to the free-volume

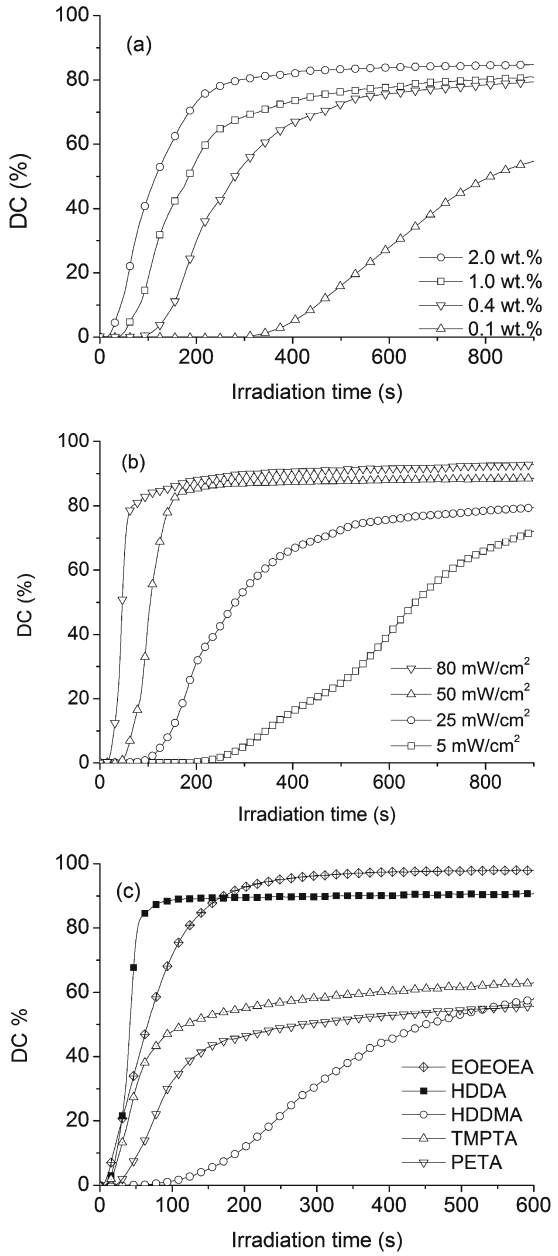

Fig. 6 The influencing factors on photopolymerization. (a) Effect of BPC2BDO concentration (I_0 = 10 mW cm^{-2}). (b) Effect of light intensity ([BPC2BDO] = 0.4 wt%). (c) Double-bond conversion of different monomers ([BPC2BDO] = 1.0 wt%, I_0 = 35 mW cm^{-2}).

effect, caused by the volume shrinkage.[2] The volume shrinkage occurred at a very fast rate of polymerization and resulted in an increase in free-volume formation, which increased the mobility of the residual double bonds and led to a higher final conversion.

Fig. 6b shows DC *versus* irradiation time plots of HDDA initiated by 0.4 wt% BPC2BDO at different light intensities. It showed similar trends to the effect of BPC2BDO concentration. The polymerization rate and final conversion increased with increase in light intensity. This was because the higher light intensity could yield more radicals which led to the increase in polymerization rate and final conversion. At the same time, more radicals yielded by the increase of light intensity could more efficiently overcome oxygen inhibition, resulting in shortening of the induction period.[37]

Table 3 Functionality, viscosity and final conversions of the monomers[a]

	Functionality	Viscosity[b] (cP)	DC_f[c] (%)
EOEOEA	1	5	97.8
HDDA	2	8	90.8
HDDMA	2	8	58.3
TMPTA	3	110	63.2
PETA	3	525	55.5

[a] The monomers were mixed with BPC2BDO with concentration of 1.0 wt%. [b] The viscosity was measured by rotation viscometer at 25 ± 1 °C. [c] DC_f represents the final double bond conversion.

The properties of the monomers would also affect the final conversions and rate of polymerization in the photopolymerization. Fig. 6c showed DC *vs.* irradiation time plots of different monomers. The functionality, viscosity and final conversions of the monomers were listed in Table 3.

The results indicated that EOEOEA and HDDA could be effectively photoinduced by BPC2BDO. The final conversion of HDDA was 90.8%, much higher than that of HDDMA (58.3%), and the rate of polymerization of HDDA was also significantly higher than that of HDDMA. These differences might be due to the α-methyl group present in the monomer which stabilizes the propagating radical.[38] The functionality of the monomer also had a strong influence on both the polymerization rate and final conversion. As the functionality increased, the viscosity of the monomer increased, with the resulting gel-effect and the higher cross-link density, which set a limit to the extent of conversion.[39] EOEOEA is a monoacrylate, so the lower initial concentration of acrylate groups lead to initially slower polymerization rate but the lower viscosity resulted in higher final conversion compared to TMPTA which is a triacrylate. While the monomer viscosity was also influenced by hydrogen bonding, contributions from extramolecular hydrogen bonding might significantly increase the viscosity of the monomer as well as affect its diffusion potential during polymerization. As the hydrogen bonding could lead to an increase of viscosity and sets a limit to the extent of conversion, the final conversion of PETA, which is also a triacrylate, was lower than that of TMPTA.

4 Conclusion

In conclusion, a benzodioxole derivative based on 4-hydroxybenzophenone and sesamol was synthesized and used as a one-component Type II photoinitiator. It was shown that the R_d of BPC2BDO in acetonitrile was proportional to light intensity. The kinetics of photopolymerization of the photoinitiator was studied by real-time infrared spectroscopy. The results showed that BPC2BDO was a more effective photoinitiator than BP/BDO, and the rate of polymerization of acrylates was

significantly higher than that of methacrylates at the same polymerization conditions, and the functionality of acrylates, concentration of BPC2BDO, and light intensity affected the polymerization rate and the final conversion.

Acknowledgements

The authors would like to thank the National Natural Science Foundation of China (20774010 and 21004047) for their financial support. This study was also supported by Doctoral Fund of Youth Scholars of Ministry of Education of China (No 20106101120005) and Science and Technology Bureau of Changzhou (CZ20110007).

References

1 J. P. Fouassier, *Photoinitiation, Photopolymerization and Photocuring*, Hanser Verlag, Munich, 1995.
2 J. F. Rabek, *Mechanisms of Photophysical Processes and Photochemical Reactions in Polymers, Theory and Applications*, Wiley, New York, 1987.
3 R. S. Davidson, *Exploring the Science, Technology and Applications of UV and EB Curing*, SITA Technology Ltd., London, 1999.
4 K. Dietliker, *Chemistry and Technology of UV and EB Formulations for Coatings, Inks and Paints*, SITA Technology Ltd, London, 1991.
5 S. P. Pappas, *UV Curing Science and Technology*, Technology Marketing Corp., Norwalk, CT, 1978.
6 Y. Yagci, S. Jockusch and N. J. Turro, *Macromolecules*, 2010, **43**, 6245.
7 N. Arsu, I. Reetz, Y. Yagci and M. K. Mishra, in *Handbook of Vinyl Polymers Radical Polymerization: Process, and Technology*, ed. M. K. Mishra and Y. Yagci, CRC Press, Boca Raton, 2009.
8 A. Ledwith and D. Purbrick, *Polymer*, 1973, **14**, 521.
9 G. Yilmaz, B. Aydogan, G. Temel, N. Arsu, N. Moszner and Y. Yagci, *Macromolecules*, 2010, **43**, 4520.
10 A. Ledwith, J. A. Bosley and M. D. Purbrick, *J. Oil Colour Chem. Assoc.*, 1978, **61**, 95.
11 A. Y. Polykarpov, S. Hassoon and D. C. Neckers, *Macromolecules*, 1996, **29**, 8274.
12 B. R. Nayak and L. J. Mathias, *J. Polym. Sci., Part A: Polym. Chem.*, 2005, **43**, 5661.
13 S. Jauk and R. Liska, *Macromol. Rapid Commun.*, 2005, **26**, 1687.
14 S. G. Cohen, A. Parola and G. H. Parsons, *Chem. Rev.*, 1973, **73**, 141.
15 M. von Raumer, P. Suppan and E. Haselbach, *Chem. Phys. Lett.*, 1996, **252**, 263.
16 T. Corrales, F. Catalina, C. Peinado and N. S. Allen, *J. Photochem. Photobiol., A*, 2003, **159**, 103.
17 N. Arsu, R. Stephen Davidson and R. Holman, *J. Photochem. Photobiol., A*, 1995, **87**, 169.
18 W. N. Albrecht and R. L. Stephenson, *Scand. J. Work, Environ. Health*, 1988, **14**, 209.
19 R. L. Bowen and H. Argentar, *J. Dent. Res.*, 1971, **50**, 923.
20 R. L. Bowen and H. Argentar, *J. Dent. Res.*, 1972, **51**, 473.
21 J. Nie and C. N. Bowman, *Biomaterials*, 2002, **23**, 1221.
22 K. D. Ahn, D. K. Han, S. H. Lee and C. W. Lee, *Macromol. Chem. Phys.*, 2003, **204**, 1628.
23 P. S. V. C. Bandyopadhyay, *PAFAI J.*, 1988, **10**, 25.
24 M. Tagashira and Y. Ohtake, *Planta Med.*, 1998, **64**, 555.
25 Q. Hu, J. Xu, S. Chen and F. Yang, *J. Agric. Food Chem.*, 2004, **52**, 943.
26 L. Jurd, V. L. Narayanan and K. D. Paull, *J. Med. Chem.*, 1987, **30**, 1752.
27 R. Joshi, M. S. Kumar, K. Satyamoorthy, M. K. Unnikrisnan and T. Mukherjee, *J. Agric. Food Chem.*, 2005, **53**, 2696.
28 E. Hodgson and R. M. Philpot, *Drug Metab. Rev.*, 1974, **3**, 231.
29 S. Shi and J. Nie, *J. Biomed. Mater. Res., Part B*, 2007, **82**, 44.
30 S. Shi and J. Nie, *J. Biomed. Mater. Res., Part B*, 2007, **82**, 487–493.
31 J. Yang, F. Xu, S. Shi and J. Nie, *Photochem. Photobiol. Sci.*, 2012, **11**, 1377.
32 W. L. F. Armarego and C. L. L. Christina, *Purification of Laboratory Chemicals*, 6th edn, 2009.
33 J. W. Stansburya and S. H. Dickens, *Dent. Mater.*, 2001, **17**, 71.
34 J. Lalevée, S. Telitel, M. A. Tehfe, J. P. Fouassier, D. P. Curran and E. Lacôte, *Angew. Chem., Int. Ed.*, 2012, **51**, 5958.
35 D. P. Curran, A. Boussonnière, S. J. Geib and E. Lacôte, *Angew. Chem., Int. Ed.*, 2012, **51**, 1602.
36 P. Xiao, J. Lalevée, X. Allonas, J. P. Fouassier, C. Ley, M. El-Roz, S. Q. Shi and J. Nie, *J. Polym. Sci., Part A: Polym. Chem.*, 2010, **48**, 5758.
37 C. Dizman, S. Ates, L. Torun and Y. Yagci, *Beilstein J. Org. Chem.*, 2010, **6**, 56.
38 G. A. O'Neil, M. B. Wisnudel and J. M. Torkelson, *Macromolecules*, 1996, **29**, 7477.
39 X. Jiang, X. Luo and J. Yin, *J. Photochem. Photobiol., A*, 2005, **174**, 165.